Honda Research Institute EU
Honda Research Institute Europe GmbH
https://www.honda-ri.de/

Extensions for the Foresighted Driver Model: Tactical Lane Change, Overtaking and Continuous Lateral Control

Florian Damerow, Benedict Flade, Julian Eggert

2016

Preprint:

This is an accepted article published in Intelligent Vehicles Symposium (IV).
The final authenticated version is available online at:
https://doi.org/10.1109/IVS.2016.7535384

Extensions for the Foresighted Driver Model: Tactical Lane Change, Overtaking and Continuous Lateral Control

Florian Damerow[1], Benedict Flade[2] and Julian Eggert[3]

***Abstract*— The *Foresighted Driver Model* (FDM) is a microscopic driver model which is based on the idea that a driver balances risk with utility. This paper deals with the modeling of advanced driving maneuvers for the FDM with a special focus on lateral positioning scenarios, such as lane changes in highway traffic. When driving at high speeds, tactical preparation for a safe lane change is of high importance. In this context, the paper presents maneuvers that allow for lane changes to be planned well in advance and carefully made without the restraint of requiring immediate action. Furthermore, the paper presents a continuous lateral control which allows driving on arbitrary paths other than the centerline, depending on the current traffic situation. Since more complex lateral maneuvers require more detailed considerations of the environment, an approach is presented to model the lane and the environmental influences. This paves the way for a modeling of variables such as lane markings, roadblocks, hard shoulders and more. Simulations illustrate how the introduced maneuvers allow successful preparation for upcoming lane changes and how traffic obstructions can be bypassed without performing a lane change but by using the continuous lateral control.**

I. Introduction

The modeling of realistic driving behavior has been a strong research area in recent years and even if there are numerous approaches targeting this problem, there are still considerable problems to solve.

On one hand driver models are widely applied to traffic simulators in order to evaluate advanced driver assistant systems (ADAS) in realistic simulation environments. On the other hand driver models are applied directly for ADAS with the target to predict the future behavior of the ego-car or other vehicles. In such a way they can be utilized to determine dangerous driving situations by analyzing and comparing the actual behavior of a driver with "how the driver should behave" and then warn to provide time to react, (e.g. [1], [2]).

In the areas of *Driver Intent Inference* and prediction of human driving behavior, one of the main problems is the prediction of spatio-temporal trajectories of drivers, especially under consideration of interactions between multiple drivers. In order to perform such a prediction of possible driver behaviors in terms of spatio-temporal trajectories, basically two different kinds of approaches exist. First, there are learning based approaches such as [3] trying to predict a traffic participants' behavior based on a large set of training data and features indicating the future behavior. Second, there are approaches using driver models such as the Intelligent Driver Model (IDM) [4] or the more general Foresighted Driver Model (FDM) [5] in a forward simulation of the current driving situation. In general, and especially if sufficient training data is available, learning based approaches perform more accurately. On the other side, particularly in the case of a highly general driver model, the model based approaches perform better in a wider range of different scenarios, especially for predicting dangerous traffic situations in which not sufficient training data is available.

In [2], a driver model based on the Intelligent Driver Model (IDM) [4] is used to determine the driving behavior in car-following scenarios by comparing the actual driving behavior with trajectory predictions for different possible maneuvers. In [1] a similar approach uses the Foresighted Driver Model (FDM) [5] to determine the lack of interaction between multiple vehicles in situations in which an interaction is necessary to avoid upcoming crashes. In both works the probability of a future maneuver is estimated by comparing the predicted trajectories with the actually sensed trajectories to estimate the current intent of the driver.

In order to increase the certainty of maneuver detection, it is highly important that the prediction models are as close as possible to the real human behavior, which is the scope of this work. Especially in highway scenarios, realistic lane changing is a highly important aspect. According to the ADAC-accident research presented in [6], lane changing and overtaking maneuvers are one of the three most frequent causes leading to a crash.

There are multiple approaches extending longitudinal driver models, e.g. IDM [2], FDM [5] or Krauss [7], by lateral maneuver possibilities, such as lane changes. In those approaches, such as the widely spread MOBIL [8] or the FDM-based model in [9], a lane change is modeled as the decision if a lane change should happen right now. But in reality, a lane change requires a preparing behavior such as adapting to the same velocity range as vehicles on the target lane, which we incorporate in this work. Furthermore, the assumption that vehicles only follow the centerline of a lane is error-prone, especially if the considered vehicle has to perform a slight evasive behavior to avoid obstacles on the side of the road.

Besides the longitudinal driver models, targeted in this paper, there are more advanced approaches assessing lane

[1]Florian Damerow is with the Control Methods and Robotics Lab, Technical University of Darmstadt, 64283 Darmstadt, Germany florian.damerow@rmr.tu-darmstadt.de

[2]Benedict Flade is with the Control Methods and Robotics Lab, Technical University of Darmstadt, 64283 Darmstadt, Germany benedict.flade@honda-ri.de

[3]Julian Eggert is with the Honda Research Institute (HRI) Europe, Carl-Legien-Str. 30, 63073 Offenbach, Germany julian.eggert@honda-ri.de

©2016 IEEE. Personal use of this material is permitted.
Permission from IEEE must be obtained for all other uses, in any current or future media, including reprinting/republishing this material for advertising or promotional purposes, creating new collective works, for resale or redistribution to servers or lists, or reuse of any copyrighted component of this work in other works.
DOI: 10.1109/IVS.2016.7535384

change behavior such as the situation assessment for automatic lane changes [10] or the polynomial based trajectory planning [11], which are computationally more demanding and not targeted for longitudinal driver models.

The paper is organized as follows. In section II we give a short introduction to the longitudinal Foresighted Driver Model as well as the lane change model introduced in [9]. Then in section III we extend the lane change model by more complex lane change variants, which include lane change preparing behavior. In section IV an additional type of risk based on the environmental structure extends the FDM. This allows us in section V to additionally perform maneuvers with continuous lateral control. Finally in section VI and VII we evaluate the models in a simulation of different traffic scenarios, conclude and give a short outlook.

II. The Foresighted Driver Model

The presented paper is a result of subsequent work on the Foresighted Driver Model introduced in [5] and the lane change model for the FDM introduced in [9]. Both works build the basis of the presented approach, in which we aim at a more realistic modeling of driving behavior, compared to the original FDM. Especially a more complex lateral behavior, starting from multi-lane-change solutions up to continuous lateral control is targeted.

The Foresighted Driver Model is a longitudinal driver model similar to the Intelligent Driver Model (IDM) [4]. But unlike the IDM, the FDM is applicable to more complex traffic scenarios such as intersections with multiple traffic participants. When developing the FDM we tried to keep the advantages of the IDM while overcoming the quite strong limitations.

The underlying idea of the FDM is to adapt a driver's behavior/velocity by finding a trade-off between utility and risk. Before going into detail, we would like to outline the general scheme of the Foresighted Driver Model. It consists of the following steps:

1) Perform a rough prediction of the traffic scene[1] considering different traffic situations, resulting in multiple predicted spatio-temporal trajectories of the ego and other involved vehicles
2) Perform an evaluation of upcoming risk based on the predicted trajectories
3) Determine the current utility cost function
4) Combine risk and utility costs into one cost function.
5) Perform a suitable velocity change such that the combined cost function is minimized by a gradient descent on the cost function

These steps 1-5 will remain valid also for the approach presented in this paper, with substantial extensions however to steps 1 and 2, to incorporate a tactical lane change as well as continuous lateral control.

[1]Here, scene refers to the actual measurable current state, whereas a situation describes one possible evolution of future states.

A. Trajectory Prediction

For the trajectory prediction we consider different driving situations, which are then combined in the risk evaluation. As described in [12], [13], [14] a situation can be defined as the relations between several (here the ego vehicle and another vehicle) traffic participants. Each situation is then defined by one prototypical behavior (here spatio-temporal trajectory) for each entity (see [12]). We always consider all of the following 3 situations in order to evaluate the driving behavior along a spatial path (see [5]):

1) Both, the ego vehicle and the considered other vehicle keep on driving with constant velocity
2) The ego vehicle keeps the velocity constant while the other vehicle performs a sharp deceleration
3) The other entity keeps the velocity constant while the ego vehicle performs a sharp deceleration

The first situation considers the main foresighted driving behavior. The second situation mainly considers the safety gap to the leading vehicle while the third situation considers the safety gap to a fast approaching vehicle from behind.

B. Risk

The risk measure used for the FDM is a simplified version of the risk evaluation presented in [15], [16], [13] and tries to estimate risk by regarding only the expected risk maxima (with peak height and width), which makes the risk evaluation computationally more efficient while retaining many of the characteristics of a full risk evaluation. For this purpose, different risk indicators are introduced for estimating the future risk function in [5].

Assuming two predicted spatio-temporal trajectories, one for the ego vehicle $\mathbf{x}_{\text{ego}}(t)$ and one for another vehicle $\mathbf{x}_{\text{other}}(t)$, as shown in Fig. 1, we calculate the Time-Of-Closest-Encounter (TCE), which is the point in time when the considered vehicles get closest along their predicted spatio-temporal trajectories,

$$\text{TCE} = \text{argmin}_t \left\| \mathbf{x}_{\text{ego}}(t) - \mathbf{x}_{\text{other}}(t) \right\|, \tag{1}$$

the Point-of-Closest-Encounter (PCE), which represents the ego vehicle position at the TCE,

$$\text{PCE} = \mathbf{x}_{\text{ego}}(\text{TCE}), \tag{2}$$

the Time-To-Closest-Encounter (TTCE) which is a Time-To-X indicator similar to the well known Time-To-Collision,

$$\text{TTCE} = \text{TCE} - t, \tag{3}$$

where t is the current time and the Distance-of-Closest-Encounter (DCE) as the minimal distance of the trajectories,

$$\text{DCE} = \min \left\| \mathbf{x}_{\text{ego}}(t) - \mathbf{x}_{\text{other}}(t) \right\|. \tag{4}$$

In general, risk can be understood as the expectation value of the costs or benefits related to a critical future event [18] and thus as the product of severity and probability of the considered event,

$$\text{risk} := \text{sev} \cdot \text{prob}. \tag{5}$$

©2016 IEEE. Personal use of this material is permitted.
Permission from IEEE must be obtained for all other uses, in any current or future media, including reprinting/republishing this material for advertising or promotional purposes, creating new collective works, for resale or redistribution to servers or lists, or reuse of any copyrighted component of this work in other works.
DOI: 10.1109/IVS.2016.7535384

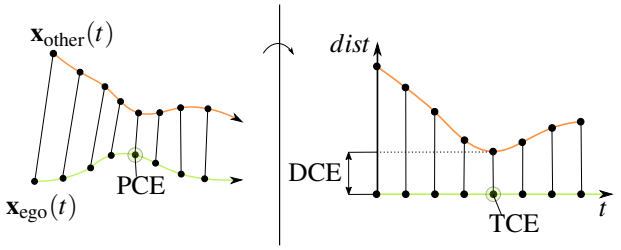


Fig. 1: Determination of risk indicators based on predicted spatio-temporal trajectories of two vehicles (see [17]).

The ego-car considers multiple other involved vehicles j. Regarding each vehicle, multiple critical events i (e.g. collision) are possible. This also incorporates the possible critical events caused by the considered three driving situations mentioned earlier. The total collision risk can then be calculated as,

$$\text{risk}^{\text{co}} = \sum_{\text{other vehicle } j} \sum_{\text{event } i} \text{risk}^{\text{co}}_{j,i}. \tag{6}$$

The probability that a collision event (co) between the ego vehicle and a vehicle j actually happens is modeled using the previously defined collision risk indicators as,

$$\text{prob}^{\text{co}}_{j,i} \sim e^{-\frac{\max(\text{DCE}_{j,i}-d^0_j,0)}{\sigma^{\text{d}}_j}} e^{-\frac{\left|\text{TTCE}_{j,i}\right|^2}{2\left(\sigma^{\text{co}}_j\right)^2}}. \tag{7}$$

The severity is modeled deterministically by the energy transfer between the two entities in case this collision event actually happens,

$$\text{sev}^{\text{co}}_{j,i} \sim S^{\text{co},0}_{j,i}[1+\alpha^{\text{co}}_j \frac{MM_j}{2(M+M_j)}(\Delta\bar{v}_{j,i})^2(1-k_j^2)] \tag{8}$$
$$\text{with } \Delta\bar{v}_{j,i} = \bar{v}(\text{TCE}_{j,i}) - \bar{v}_j(\text{TCE}_{j,i}).$$

with ego velocity $\bar{v}$ and other velocities $\bar{v}_j$. For a detailed explanation see [5].

Using (6), (7) and (8) the total collision risk[2] is,

$$\text{risk}^{\text{co}}(t,v) = \sum_j \sum_i \text{sev}^{\text{co}}_{j,i} \cdot \text{prob}^{\text{co}}_{j,i}. \tag{9}$$

For simulations, the parameters used here, such as the weighting and uncertainty parameters α^{co}_j, $S^{\text{co},0}_{j,i}$, σ^{d}_j and σ^{co}_j, the minimal allowed distance d^0_j, the restitution factor k_j or the masses of the ego and other vehicles M and M_j have been chosen identical to [5].

As shown in [5], other types of risk, such as loosing control when driving too fast through a curve, can easily be integrated into this risk measure in a similar way.

C. Balancing of risk and utility

As already mentioned, the Foresighted Driver Model is based on the idea of finding a trade-off between risk and utility, which we determine by performing a gradient descent on the velocity minimizing a cost function including both, a risk and a utility term,

$$\frac{\text{d}v}{\text{d}t} = \frac{\text{d}v}{\text{d}t}^{\text{utility}} + \frac{\text{d}v}{\text{d}t}^{\text{risk}}, \tag{10}$$

where the utility term is similar to the "free-driving" term of the IDM,

$$\frac{\text{d}v}{\text{d}t}^{\text{utility}} = a^{\text{free}}\left(1-\left(\frac{v}{V}\right)^{\beta}\right). \tag{11}$$

The risk term is simply based on the weighted risk gradient as,

$$\frac{\text{d}v}{\text{d}t}^{\text{risk}} = -\gamma \frac{\text{d risk}(t,v)}{\text{d}v}. \tag{12}$$

The underlying minimized longitudinal cost function (see [5]) is thus

$$\text{Cost}(t,v) = -a^{\text{free}}\left(v - v\frac{\left(\frac{v}{V}\right)^{\beta}+\beta V}{\beta+1}\right) + \gamma\,\text{risk}(t,v). \tag{13}$$

Again the used free driving parameters such as the desired velocity V and the acceleration defined by a^{free} and β are chosen as in [5].

D. Lane Change Model

The cost function (13), as well as the cost minimizing velocity adaptation (10) are so far only defined longitudinally along one given spatial path. In [9] the longitudinal model is extended to allow lateral lane changes. This lane change model is realized by constructing further possible paths, namely one path for driving on each accessible lane.

We then slightly extend the cost function for the "multi-path"-case with additional costs $\Delta(l, l^{\text{current}})$ for changing the lane, comparable to the "cost of actuation" found in LQR controllers. In cases in which the costs for two possible paths are quite similar, those additional costs hinder the system to change lane with high frequency:

$$\text{Cost}(t,v,l) := -a^{\text{free}}\left(v - v\frac{\left(\frac{v}{V}\right)^{\beta}+\beta V}{\beta+1}\right) + \gamma\,\text{risk}(t,v,l)$$
$$+\Delta(l,l^{\text{current}}), \tag{14}$$

where $\text{risk}(t,v,l)$ is calculated according to (9) for a certain lane or path l. l denotes the evaluated lane/path and l^{current} the currently selected lane/path.

For each path we then determine the costs for a differential change in velocity, which provides a cost matrix as shown in table I. Finally, we choose the path with minimal costs and perform the velocity adaptation with the longitudinal FDM. The cost matrix in table I can be understood as a discrete decision on "driving slower on the current lane" vs "driving faster on the current lane" vs "driving slower on the other lane" vs "driving faster on the other lane".

The longitudinal driver model [5] as well as the simple lane change model [9] based on the discrete path selection build the basis of the following lateral extensions of the FDM towards more complex lateral behavior options. The

[2](9) is an approximation of the accumulated time continuous risk model introduced in [15].

©2016 IEEE. Personal use of this material is permitted.
Permission from IEEE must be obtained for all other uses, in any current or future media, including reprinting/republishing this material for advertising or promotional purposes, creating new collective works, for resale or redistribution to servers or lists, or reuse of any copyrighted component of this work in other works.
DOI: 10.1109/IVS.2016.7535384

$\text{Cost}(t,v,l)$	l^{current}	l^{other}
$v+\Delta v$	1.1	0.3
$v-\Delta v$	0.7	**0.1**

TABLE I: Exemplary cost matrix for two possible lanes (see [9]). It can be seen that in this case l^{other} would be chosen as the future desired lane/path while the velocity adaptation will reduce the velocity along this path.

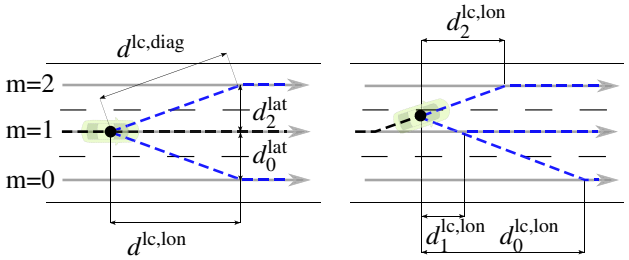


Fig. 2: Ego-car on a three-lane road with full centerline to centerline lane changes (left) and lane changes starting from arbitrary lateral positions (right).

integrated risk evaluation in the FDM allows a parallel and continuous consideration of multiple possible maneuvers. Similar to the idea of model predictive control (mpc), the decision of the current driving maneuver can be adapted at any time. As shown in Fig. 2, the possible future paths are constructed by using the centerline of each accessible lane and an on-ramp part, which we define in the following. We first determine the duration of a lane change (lc) starting from any given position to a target lane m as

$$t_m^{\text{lc}} = t^{\text{lc},0} \cdot \frac{d_m^{\text{lat}}}{d^{\text{lane}}}, \tag{15}$$

where d_m^{lat} is the lateral distance to the centerline of the target lane, d^{lane} the distance between two neighboring lanes and $t^{\text{lc},0}$ the desired duration of a single lane change from centerline to centerline.

The actual length of the ramp-on part of the path is then given by,

$$d_m^{\text{lc,diag}} = v \cdot t_m^{\text{lc}}, \tag{16}$$

thus resulting for the longitudinal distance

$$d_m^{\text{lc,lon}} = \sqrt{{d_m^{\text{lc,diag}}}^2 - {d_m^{\text{lat}}}^2}. \tag{17}$$

III. Modeling of more realistic lane change maneuvers

The FDM can be used to model single-lane traffic as well as multi-lane traffic. Anticipatory driving requires an evaluation of the current situation in conjunction with a prediction of future situations. In this context, a tactical preparation for a safe lane change is of high importance. Up to now, the ego-car only takes lane changes into account that are performed immediately. In a next step, we aim to allow not only immediate lane changes but also lane changes that are planned well in advance. An earlier decision in favor of a lane change allows a preparation in terms of a foresighted speed adjustment.



Fig. 3: Two-lane road scenario showing the ego-car approaching two slower cars. The vector in front of the respective vehicle is proportional to its speed.

A. Tactical Lane Change

Considering a road with p-lanes, the ego-car can choose to stay on the current lane or to switch to one of the $p-1$ alternative lanes. Fig. 3 depicts a case in which the ego-car approaches other traffic participants on a two-lane road, which results in a 2×2-cost-matrix. As the ego-car approaches the slower car 2, the risk increases and thus staying on the current lane results in a speed reduction. Owing to car 1 on the adjacent lane, also an immediate lane change leads to a deceleration.

In such a situation, a human driver considers a third option in which the lane change isn't performed immediately, but performed as soon as the car on the adjacent lane has been passed. An early consideration of a so called *tactical lane change* (tlc) allows a speed adjustment and thereby a preparation for an upcoming lane change.

In the current lane change model of the FDM, only immediate but no planned lane changes are provided, which is why the behavior of the simulated ego-car may differ strongly from the behavior of a human driver. We therefore model the tactical lane change path which will be added to the cost matrix. In this way, the ego-car is able to consider and prepare lane changes that are not started immediately.

The modeling of this maneuver is based on the idea that a driver remains on the current lane n until the reference car on the adjacent lane m is passed and until a safety distance is achieved, so that a safe lane change is possible. In order to determine the path of the tactical lane change, the distance traveled on the current lane before the lane change starts, as well as the longitudinal distance traveled while performing the lane change have to be estimated. For this purpose, we formulate the longitudinal kinematic equations of the ego-car and each other car as

$$p_{\text{ego}} + v_{\text{ego}} \cdot \Delta t^{\text{tlc}} = p_{\text{other}} + v_{\text{other}} \cdot \Delta t^{\text{tlc}} + d^{\text{safe}} \tag{18}$$

with the positions p_{ego} and p_{other} of the two considered cars as well as their velocities v_{ego} and v_{other}. Furthermore, a longitudinal safety distance d^{safe} is taken into account[3]. For the estimated duration t^{tlc} on the original lane and the resulting traveled distance, we then get

$$\begin{aligned} \Delta t^{\text{tlc}} &= \frac{p_{\text{other}} + d^{\text{safe}} - p_{\text{ego}}}{v_{\text{ego}} - v_{\text{other}}}, \quad \text{if} \quad p_{\text{ego}} < p_{\text{other}} + d^{\text{safe}} \\ \Delta t^{\text{tlc}} &= 0, \quad \text{if} \quad p_{\text{ego}} > p_{\text{other}} + d^{\text{safe}}, \end{aligned} \tag{19}$$

thus resulting in the estimated traveled distance before the lane change

$$d^{\text{tlc}} = v_{\text{ego}} \cdot \Delta t^{\text{tlc}}. \tag{20}$$

In this regard, Δt^{tlc} describes the required time until the lane

[3]Here, the distance is formulated as a function of the ego-car velocity.

©2016 IEEE. Personal use of this material is permitted.
Permission from IEEE must be obtained for all other uses, in any current or future media, including reprinting/republishing this material for advertising or promotional purposes, creating new collective works, for resale or redistribution to servers or lists, or reuse of any copyrighted component of this work in other works.
DOI: 10.1109/IVS.2016.7535384

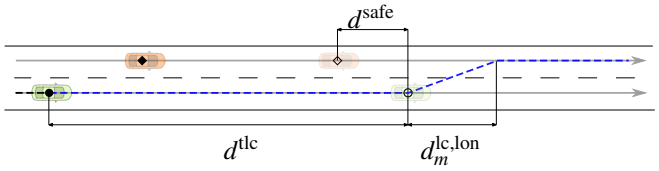


Fig. 4: Path of a possible tactical lane change maneuver. The current positions of the ego-car and the reference car are depicted with a filled circle and a filled diamond. The positions at the time of the predicted lane change are illustrated with blank symbols.

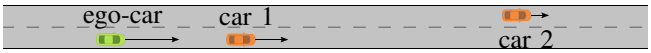


Fig. 5: Two-lane road scenario showing the ego-car approaching a slower car 1 on the same lane. The vector in front of the respective vehicle is proportional to its speed.

change. For $\Delta t^{\text{tlc}} = 0$, the tactical lane change is equivalent to an immediate lane change as the safety distance is already maintained. The actual car dimensions can be taken into account by adapting the car positions in (18). Fig. 4 illustrates the tactical lane change path, which is based on the distance d^{tlc} prior to the lane change.

B. Overtaking

Regarding highway traffic, a great majority of the lane changes are part of an overtaking maneuver in which the driver aims to return to the current lane. Fig. 5 depicts a scenario in which the ego-car aims to perform the overtaking process before the gap between the followed car 1 and car 2 on the adjacent lane closes. In such a situation, a human driver is either expected to decelerate while staying on the current lane n or expected to change lanes so that car 1 can be passed before the gap to car 2 is too small. In order to capture the entire overtaking processes in terms of risk and utility, we now extend the model to take trajectories into account that not only lead to the adjacent lane *but also lead back to the current lane*.

Similarly to the tactical lane change, the kinematic equations for the overtaking maneuver have to be formulated. In this case, the time for the first lane change to lane m, which initiates the maneuver, has to be taken into account. With the positions and velocities of the ego-car and the reference car, we then get

$$p_{\text{ego}} + d_m^{\text{lc,lon}} + v_{\text{ego}} \cdot \left(\Delta t^{\text{ot}} - \Delta t_m^{\text{lc}}\right) = p_{\text{other}} + v_{\text{other}} \cdot \Delta t^{\text{ot}} + d^{\text{safe}}. \tag{21}$$

Solving the equation for Δt^{ot} leads to

$$t^{\text{ot}} = \frac{p_{\text{other}} + d^{\text{safe}} - p_{\text{ego}} - d_m^{\text{lc,lon}} + v_{\text{ego}} \cdot \Delta t_m^{\text{lc}}}{v_{\text{ego}} - v_{\text{other}}} \tag{22}$$

and thus

$$\begin{aligned} d^{\text{pass}} &= v_{\text{ego}} \cdot \left(\Delta t^{\text{ot}} - \Delta t_m^{\text{lc}}\right), \quad \text{if} \quad \Delta t^{\text{ot}} > \Delta t_m^{\text{lc}} \\ d^{\text{pass}} &= 0, \qquad\qquad \text{if} \quad \Delta t^{\text{ot}} < \Delta t_m^{\text{lc}}. \end{aligned} \tag{23}$$

It is important to stress that Δt^{ot} does not describe the duration of the whole overtaking maneuver but the required time until the second lane change can be performed. In order to illustrate the overtaking process, Fig. 6 shows the ego-car and the reference car at the beginning of the maneuver (filled symbols) and at the moment at which the safety distance is maintained (blank symbols).

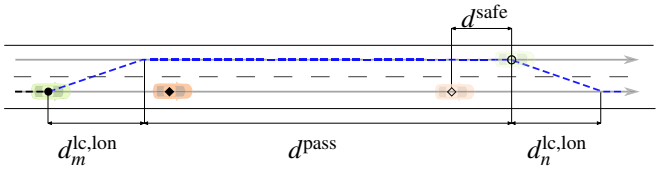


Fig. 6: Path of a potential overtaking maneuver. The current positions of the ego-car and the reference car are depicted with a filled circle and a filled diamond. The positions at the time of the predicted lane change are illustrated with blank symbols.

IV. Structural Risk

As explained in section II, the cost function (14) is extended by an additional cost term $\Delta(l, l^{\text{current}})$ in order to avoid frequent lane changes. This cost term acts basically as a cost threshold. Therefore, a lane change is only performed if the costs for a lane change are at least the threshold lower than the costs for staying on the current lane.

Here we target more complex maneuvers such as realistic lane changes, introduced in section III, or even a continuous lateral control. Furthermore, we argue that the cost threshold used in [9] results from risk caused by structural elements. As a result we model the lateral costs as structural risk and combine it with the car-to-car collision risk.

$$\text{Cost}(t, v, l) = \text{Cost}^{\text{utility}}(t, v) + \text{Cost}^{\text{risk}}(t, v, l), \tag{24}$$

where

$$\begin{aligned} \text{Cost}^{\text{risk}}(t, v, l) &= \gamma\ \text{risk}^{\text{co}}(t, v, l) \\ &+ \rho\ \text{risk}^{\text{struct}}(t, l). \end{aligned} \tag{25}$$

Here l denotes not only paths on different lanes, but any spatial path that differs in its lateral component.

As shown in Fig. 7 we model different instantaneous structural risks by Gaussians or other simple functions of the lateral position p_{lat} on the road. Each of those risks are denoted as $g_k(p_{\text{lat}})$. Here we model e.g. certain risks for driving on the mid-lane markings (Fig. 7 top, left), driving over the road boundary markings (top, middle) or driving on the hard shoulder (bottom, left). More risk types such as roadblocks or even traffic rules are also conceivable. By combining the single structural risks we gather a structural risk landscape, which in general has its minima along the centerlines of each lane, increases for driving inbetween lanes and approaches high values at the road boundary.

Similar to the idea of discounting the collision risk with an increase in DCE, we also discount structural risks further away. This accounts for an increase of uncertainty in positioning and decision making. The full structural risk is then

$$\text{risk}^{\text{struct}}(t, l) = \int_c \sum_k g_k(p_l^{\text{lat}}(c)) \cdot \mathrm{e}^{-\left(\frac{p_l^{\text{lon}}(c)}{\sigma^{\text{lon}}}\right)^2} \mathrm{d}c \tag{26}$$

©2016 IEEE. Personal use of this material is permitted.
Permission from IEEE must be obtained for all other uses, in any current or future media, including reprinting/republishing this material for advertising or promotional purposes, creating new collective works, for resale or redistribution to servers or lists, or reuse of any copyrighted component of this work in other works.
DOI: 10.1109/IVS.2016.7535384

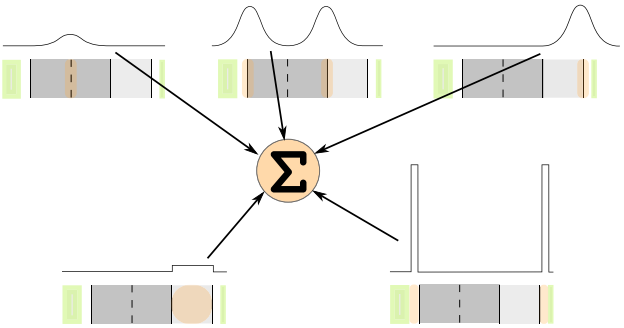


Fig. 7: Modeling of instantaneous structural risk for a multi-lane road.

where the vehicle path is parametrized by a variable c. We can then extract the path's longitudinal and lateral position $p_l^{\text{lon}}(c)$ and $p_l^{\text{lat}}(c)$ relative to a reference line of the road (e.g. the total right road boundary). σ^{lon} is chosen so that $\mathrm{e}^{-\left(p_l^{\text{lon}}(c)/\sigma^{\text{lon}}\right)^2} \approx 0$ for the maximal length of the path. The structural risk is dependent on the current time t, as it implicitly defines the starting point of the evaluated path.

V. Continuous Lateral Control

The FDM is a driver model that allows to simulate longitudinal as well as multi-lane traffic. The latter is achieved by comparing trajectories that lead from the lane center of the current lane to the lane center of another lane.

Depending on the environment and the traffic situation, it can be reasonable to perform an evasive maneuver instead of a full lane change. In the following we present a continuous lateral control which not only allows driving at the lane center but also driving on paths that deviate from the center. This can be achieved by analyzing whether a slight deviation to the left or right can improve the driving situation by means of risk and utility.

Currently, the longitudinal path is based on the centerline of the current lane, assuming that a driver aims to drive at the lane center. With regard to a continuous lateral control, we dismiss this assumption, allowing shifted paths to be considered. To implement this, we define an offset o^{clc}, describing the lateral distance between the current longitudinal path CLC^{mid} and the shifted paths CLC^{left} and CLC^{right}.

In order to follow such a shifted path, a path change analogous to a lane change has to be performed. According to section II-D, we get

$$t^{\text{clc}} = t^{\text{lc},0} \cdot \frac{o^{\text{clc}}}{d^{\text{lane}}} \tag{27}$$

$$d^{\text{clc,diag}} = v \cdot t^{\text{clc}} \tag{28}$$

$$d^{\text{clc,lon}} = \sqrt{{d^{\text{clc,diag}}}^2 - {o^{\text{clc}}}^2}. \tag{29}$$

In this case, t^{clc} describes the time needed for reaching the shifted path. In order to illustrate the equations, Fig. 8 depicts a situation in which the ego-car has already chosen a deviated path.

It should be noted that the continuous lateral control provides gradual optimization. The offset accounts as a step-width in the continuous optimization over time and should

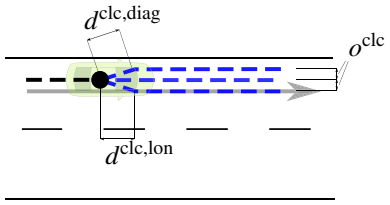


Fig. 8: Ego-Car evaluating the three possibilities resulting from the continuous lateral control.

be chosen suitably small to allow a dense coverage of the road. The case that a possible path departs from the road does not pose any problems, as an unsuitable path results in disproportionate high costs and will thus not be selected.

VI. Results on Different Scenarios

A. Tactical lane change

In order to illustrate the introduced maneuvers, we first apply our approach to a highway scenario in which the ego-car approaches two other traffic participants. At the beginning of the simulation, the ego-car $v_{\text{ego}} = 23\ \frac{\text{m}}{\text{s}}$ approaches another car (2) ($v_{\text{other},2} = 16.5\ \frac{\text{m}}{\text{s}}$) on the same lane. A third car (1) ($v_{\text{other},1} = 19\ \frac{\text{m}}{\text{s}}$) is located on the adjacent lane. The desired free driving velocity of the ego-car amounts to $V_{\text{ego}} = 26\ \frac{\text{m}}{\text{s}}$.

Fig. 9 a) illustrates the scenario for $t = 8.0$ s in its first row. An evaluation of the cost matrix (table II) shows that an immediate lane change leads to the highest costs as a collision with car 1 is likely. Also staying on the current lane creates costs as the preceding vehicle poses a risk. In both cases, a deceleration is preferable. Another option is the tactical lane change which, pursuant to the cost matrix, results in the lowest costs. This is due to the fact that the collision risks with both cars can be kept low and the utility high, as no deceleration is needed. The lane change is planned to be performed not before a safety distance to car 1 is maintained but prior to a possible collision with car 2. In this case an acceleration is recommended.

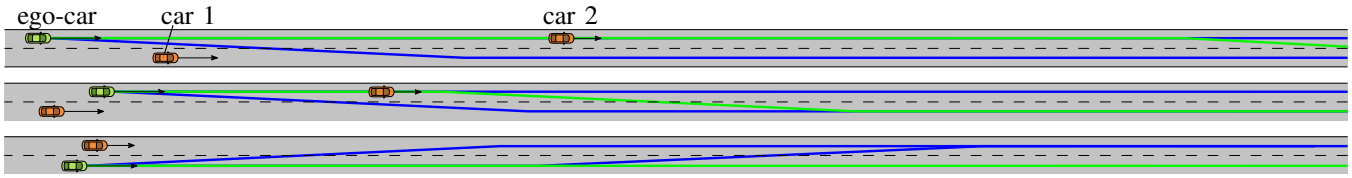
	Longitudinal	*Immed. Lane Change*	*Tactical Lane Change*
$v+\Delta v$	2.39	426.46	**0.20**
$v-\Delta v$	1.80	396.42	0.23

TABLE II: Cost matrix of the highway scenario under consideration of a tactical lane change for $t = 8$ s.

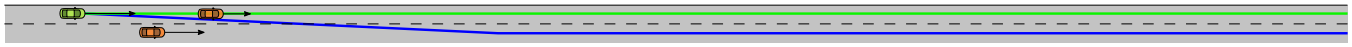
During the simulation, the cost matrix is evaluated every 0.4 s whereby the ego-car chooses regularly the path that results in the lowest costs. In the second row of Fig. 9 a), the simulation after 14 seconds is shown with a moving camera. The ego-car has passed the vehicle on the adjacent lane and is now located between car 1 and car 2. The cost matrix for $t = 14.0$ s (table III) shows that once again, the tactical lane change in conjunction with an acceleration leads to the lowest costs. While the costs from the longitudinal path trace back to car 2, the costs from the lane change path are caused by car 1. After another 6 seconds ($t = 20$ s), the ego-car has successfully performed the lane change.

In order to investigate the impact of the tactical lane change, we simulate the same scenario without the consid-

©2016 IEEE. Personal use of this material is permitted.
Permission from IEEE must be obtained for all other uses, in any current or future media, including reprinting/republishing this material for advertising or promotional purposes, creating new collective works, for resale or redistribution to servers or lists, or reuse of any copyrighted component of this work in other works.
DOI: 10.1109/IVS.2016.7535384



(a) Scenario with consideration of immediate and tactical lane change for $t = [8, 14, 20]$ s with moving camera (top to bottom).



(b) Scenario with only consideration of immediate lane change for $t = 35$ s.

Fig. 9: Highway scenario showing the ego-car behavior at different moments in time with chosen path in green and considered paths in blue.

	Longitudinal	*Immed. Lane Change*	*Tactical Lane Change*
$v+\Delta v$	88.14	59.84	**0.16**
$v-\Delta v$	78.22	74.44	0.19

TABLE III: Cost matrix of the highway scenario under consideration of a tactical lane change for $t = 14$ s.

eration of a tactical lane change path. Fig. 9 b) shows the scenario for after 35 seconds. The ego-car ($v_{\text{ego}} = 16.6\ \frac{\text{m}}{\text{s}}$) has adjusted to the speed of the preceding car 2 ($v_{\text{other,2}} = 16.5\ \frac{\text{m}}{\text{s}}$). Due to the reduced velocity, the gap between car 1 and car 2 closed before a lane change was possible so that the ego-car has to wait until car 1 passed car 2.

In Fig. 10 the velocity profiles of both cases are compared. The advantage of the tactical lane change can be clearly identified, as the profile smoothly approaches the desired free driving velocity.

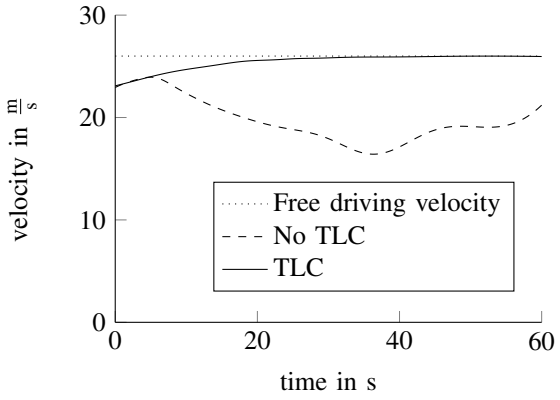


Fig. 10: Ego-car velocity profiles for the highway scenario with and without consideration of a tactical lane change and target velocity for free driving.

B. Continuous Lateral Control

In the second scenario, we consider a road with parked cars. With regard to risk and utility, parked cars are modeled with velocity $v_{\text{parked}} = 0.0\ \frac{\text{m}}{\text{s}}$. Fig 11 depicts the initial condition in its top row. Due to the imminent risk, the current longitudinal path leads to a significant deceleration.

Using the continuous lateral control, the situation can be improved. In this initial state, the middle path CLC^{mid} is equivalent to the centerline of the one-lane road. We see from table IV that a deviation to the left causes the lowest costs. This is due to the fact that the risk and thus the costs decrease with increasing lateral distance from the parked cars. The structural risk costs, caused by a deviation to the left, are equal to the costs of a deviation to the right.

	CLC^{left}	CLC^{mid}	CLC^{right}
$v+\Delta v$	0.05 (0.03)	0.23 (0.00)	0.82 (0.03)
$v-\Delta v$	**0.04** (0.03)	0.20 (0.00)	0.69 (0.03)

TABLE IV: Cost matrix of the continuous lateral control scenario for $t = 0$ s. The structural risk is additionally indicated in brackets.

The second row of Fig. 11 shows the scenario for $t = 4.0$ s. By now, the ego-car has chosen a path with a sinistral deviation of 0.76 m from the centerline. The corresponding cost matrix is shown in table V. It can be seen that both shifted paths lead to higher costs than the current path. A shift to the right increases the collision risk whereas a shift to the left results in a greater structural risk, caused by the left roadside border. For comparison purposes, the path based on the centerline is added to the cost matrix. It can be seen that driving in the middle of the lane leads to significantly higher costs, caused by the collision risk. After 65 seconds,

	CLC^{left}	CLC^{mid}	CLC^{right}	*Centerline*
$v+\Delta v$	0.86 (0.85)	**0.45** (0.33)	0.80 (0.10)	73.80 (0.00)
$v-\Delta v$	0.87 (0.85)	**0.45** (0.33)	0.79 (0.10)	73.47 (0.00)

TABLE V: Cost matrix of the continuous lateral control scenario for $t = 4.0$ s. The structural risk is additionally indicated in brackets.

the ego-car has passed the parked cars and is now back on the centerline. In order to illustrate the lateral optimization, the bottom row of Fig. 11 shows the driving profile.

VII. Discussion

In this paper we introduced extensions to the Foresighted Driver Model that allow for lane changes to be planned well in advance and carefully made without the restraint of requiring immediate action. Thereby the FDM is able to recognize potential hazards and to launch suitable countermeasures at an early stage.

Simulations showed that the consideration of a tactical lane change has a positive influence on the proposed velocity profile and on the involved risks. Furthermore, it could be demonstrated that the introduced continuous lateral control provides a useful extension in cases where a lane change is not reasonable or possible. The continuous lateral control not only allows driving at the lane center but also driving on paths that deviate from the center, depending on the current traffic situation. Thus the FDM not only balances

©2016 IEEE. Personal use of this material is permitted.
Permission from IEEE must be obtained for all other uses, in any current or future media, including reprinting/republishing this material for advertising or promotional purposes, creating new collective works, for resale or redistribution to servers or lists, or reuse of any copyrighted component of this work in other works.
DOI: 10.1109/IVS.2016.7535384

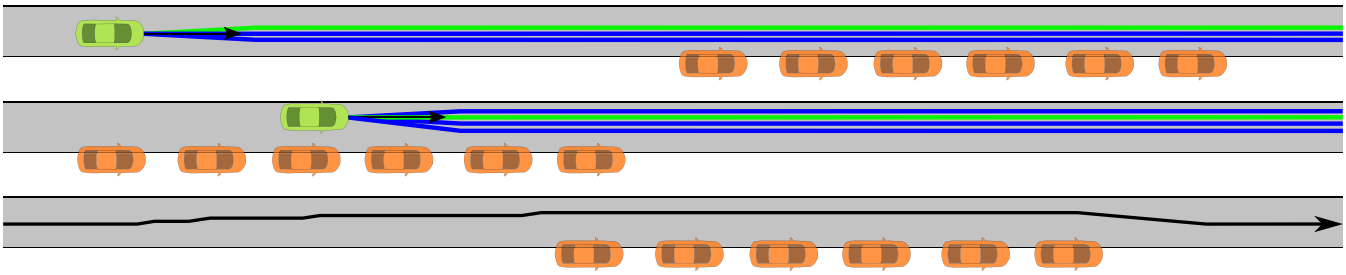


Fig. 11: Scenario with parked cars demonstrating the continuous lateral control at different moments in time with chosen path in green and considered paths in blue. Scenario for $t = 0$ s (top), $t = 4$ s (center) and the driving profile of the ego-car (bottom).

longitudinal risk with utility (expressed by the velocity) but also lateral risk caused by other traffic participants with road structure or environmental influences.

Straightforward extensions for the continuous lateral control are given by not only taking two shifted paths into account but a multitude of paths that are covering the entire road profile. In this way, instead of approaching a local minimum step by step, the continuous lateral control helps to find a global optimum right away. Nevertheless, the evaluation of a higher number of paths should be considered with caution as the evaluation of a large number of paths can be computationally intensive. A reasonable field of application is collision avoidance in near emergency or collision mitigation cases. In case of an imminent collision, the evaluation of a high number of shortened paths can present a useful collision avoidance strategy.

The tactical lane change maneuver aims at performing a lane change as soon as a safety distance is achieved. In a further step, paths with a tactical lane change that are independent of a reference car can be analyzed. This could be implemented by using a sampling approach in which skilfully selected paths are evaluated that differ on the distance to the lane change.

Furthermore, there is no limit to the combination of the maneuvers. As shown in the overtaking example, an immediate lane change can be combined with a tactical lane change that leads back to the current lane. Likewise, paths with an immediate lane change plus a tactical lane change that does not lead back to the current lane but to another lane offer room for further extensions.

In its current form, the strength of the tactical lane change and of the overtaking can only be exploited when driving in proximity to the desired free cruising velocity. Scenarios such as congested traffic may be problematic. This is due to the chosen prediction model, which assumes near constant velocities. In such scenarios, the velocities may change strongly in the course of a tactical lane change or an overtaking maneuver. Even if a potential variation of the velocity is considered when modeling the tactical lane change or overtake path, the evaluation of the risk is still based on the current velocity. To address this concern, the consideration of a velocity profile instead of a constant value while calculating the risk presents one option. This may improve the prediction, which is of great advantage, as only those who are able to predict are able to be foresighted.

References

[1] F. Damerow and J. Eggert, "Spatio-temporal Trajectory Similarity and it's Application to Situation Classification and the Evaluation of Lack of Interaction," in *IEEE Intelligent Vehicles Symposium (IV)*, 2016, p. submitted.

[2] M. Liebner, F. Klanner, M. Baumann, C. Ruhhammer, and C. Stiller, "Velocity-Based Driver Intent Inference at Urban Intersections in the Presence of Preceding Vehicles," *IEEE Intelligent Transportation Systems Magazine*, vol. 5, no. 2, pp. 10–21, jan 2013.

[3] S. Klingelschmitt and J. Eggert, "Using Context Information and Probabilistic Classification for Making Extended Long-Term Trajectory Predictions," in *IEEE Conference on Intelligent Transportation Systems (ITSC)*, 2015, pp. 705 – 711.

[4] M. Treiber, A. Hennecke, and D. Helbing, "Congested Traffic States in Empirical Observations and Microscopic Simulations," *Physical Review*, vol. 62, pp. 1805–1824, 2000.

[5] J. Eggert, F. Damerow, and S. Klingelschmitt, "The Foresighted Driver Model," in *IEEE Intelligent Vehicles Symposium (IV)*. IEEE, jun 2015, pp. 322–329.

[6] T. Unger, "ADAC Unfallforschung - Junge Fahrer 2012," ADAC Technik Zentrum Landsberg / Lech, Tech. Rep., 2012.

[7] S. Krauß, "Microscopic modeling of traffic flow: Investigation of collision free vehicle dynamics," Ph.D. dissertation, Universität zu Köln, 1998.

[8] A. Kesting, M. Treiber, and D. Helbing, "General Lane-Changing Model MOBIL for Car-Following Models," *Transportation Research Record: Journal of the Transportation Research Board*, vol. 1999, no. 1, pp. 86–94, 2007.

[9] J. Eggert and F. Damerow, "Complex Lane Change Behavior in the Foresighted Driver Model," in *IEEE Conference on Intelligent Transportation Systems (ITSC)*, 2015, pp. 1747–1754.

[10] R. Schubert, K. Schulze, and G. Wanielik, "Situation assessment for automatic lane-change maneuvers," *Intelligent Transportation Systems, IEEE Transactions on*, vol. 11, no. 3, pp. 607–616, 2010.

[11] I. Papadimitriou and M. Tomizuka, "Fast lane changing computations using polynomials," in *American Control Conference, 2003. Proceedings of the 2003*, vol. 1. IEEE, 2003, pp. 48–53.

[12] F. Damerow and J. Eggert, "Risk-Aversive Behavior Planning under Multiple Situations with Uncertainty," in *IEEE Conference on Intelligent Transportation Systems (ITSC)*, 2015, pp. 656–663.

[13] J. Eggert, S. Klingelschmitt, and F. Damerow, "The Foresighted Driver: Future ADAS Based on Generalized Predictive Risk Estimation," in *FAST-zero 2015 Symposium*, 2015.

[14] S. Klingelschmitt, F. Damerow, and J. Eggert, "Managing the Complexity of Inner-City Scenes: An Efficient Situation Hypotheses Selection Scheme," in *IEEE Intelligent Vehicles Symposium (IV)*. IEEE, 2015, pp. 1232 – 1239.

[15] J. Eggert, "Predictive risk estimation for intelligent ADAS functions," in *IEEE Conference on Intelligent Transportation Systems (ITSC)*. IEEE, oct 2014, pp. 711–718.

[16] F. Damerow and J. Eggert, "Balancing Risk against Utility: Behavior Planning using Predictive Risk Maps," in *IEEE Intelligent Vehicles Symposium (IV)*. IEEE, 2015, pp. 857 – 864.

[17] ——, "Predictive risk maps," in *IEEE Conference on Intelligent Transportation Systems (ITSC)*. IEEE, 2014, pp. 703–710.

[18] ISO31000, "Risk management - Principles and Guidelines," *International Organization for Standardization, Geneva, Switzerland*, 2009.

©2016 IEEE. Personal use of this material is permitted.
Permission from IEEE must be obtained for all other uses, in any current or future media, including reprinting/republishing this material for advertising or promotional purposes, creating new collective works, for resale or redistribution to servers or lists, or reuse of any copyrighted component of this work in other works.

DOI: 10.1109/IVS.2016.7535384